# Towards Illumination-invariant 3D Reconstruction using ToF RGB-D Cameras Supplementary Material

Christian Kerl[1], Mohamed Souiai[1], Jürgen Sturm[2], and Daniel Cremers[1]

[1]Technische Universität München, {christian.kerl,mohamed.souiai,cremers}@in.tum.de
[2]metaio GmbH, juergen.sturm@metaio.com

## 1. Introduction

The detailed procedure for solving problem $E(\mathcal{U}^k, \mathcal{S})$ is illustrated in Algorithm 1. Note that the point-wise constraints in

---

**Algorithm 1** Primal-Dual Solver for Sub-Problem $\mathbf{argmin}_{\mathcal{U}} E(\mathcal{U}, \mathcal{S}^k)$

---

Input: $\mathcal{S}^k$
Initialize $\mathcal{U}^0$
  **for** $n = 0, 1, 2, ...$ **do**
  $\mathcal{P}(\boldsymbol{x})^{n+1} = \Pi_1 \left[\mathcal{P}(\boldsymbol{x})^n + \tau \nabla \tilde{\mathcal{U}}(\boldsymbol{x})^n\right]$
  $\mathcal{U}(\boldsymbol{x})^{n+1} = \Pi_2 \left[\mathcal{U}(\boldsymbol{x})^n - \sigma \left(\mathcal{S}(\boldsymbol{x})^k(\mathcal{C}(\boldsymbol{x}) - \mathcal{S}(\boldsymbol{x})^k\mathcal{U}(\boldsymbol{x})^n) + \mathcal{G}(\boldsymbol{x})^\mathsf{T}(\mathcal{A} - \mathcal{G}(\boldsymbol{x})\mathcal{U}(\boldsymbol{x})^n) - \nabla^\mathsf{T}\mathcal{P}(\boldsymbol{x})^{n+1}\right)\right]$
  $\tilde{\mathcal{U}}(\boldsymbol{x})^{n+1} = 2\mathcal{U}(\boldsymbol{x})^{n+1} + \mathcal{U}(\boldsymbol{x})^n$
  **end for**

---

energy (23) are handled by orthogonal projectors $\Pi_1$ and $\Pi_2$ which reproject the primal and dual variables in the respective constraint sets by the following clipping operations:

$$\Pi_1\left(\mathcal{P}(\boldsymbol{x})\right) = \frac{\mathcal{P}(\boldsymbol{x})}{\max\{1, |\mathcal{P}(\boldsymbol{x})|\}} \tag{1}$$

and

$$\Pi_2\left(\mathcal{U}(\boldsymbol{x})\right) = \max\{0, \min\{\mathcal{U}(\boldsymbol{x}), 1\}\}. \tag{2}$$

The step sizes $\sigma$ and $\tau$ can be chosen according to [1]. Furthermore the inner optimization problem is performed point-wise. Hence the algorithm can be run in parallel for each pixel $\boldsymbol{x} \in \Omega$. The gradient operator $\nabla$ is a linear operator and the $\nabla^\mathsf{T}$ denotes its adjoint operator. Similarly the inner optimization problem $E(\mathcal{U}^k, \mathcal{S})$ for a fixed $\mathcal{U}^k$ can be solved as in Algorithm 2. Where $\Pi_3$ is the orthogonal projector into the respective constraint sets *i.e.*:

$$\Pi_3\left(\mathcal{S}(\boldsymbol{x})\right) = \max\{0, \mathcal{S}(\boldsymbol{x})\}. \tag{3}$$

The gradient operator $\nabla$ used in Algorithm 1 is a linear operator which calculates the derivatives point-wise and can be written as follows:

$$\nabla = \begin{bmatrix} \nabla_x & & \\ \nabla_y & & \\ & \nabla_x & \\ & \nabla_y & \\ & & \nabla_x \\ & & \nabla_y \end{bmatrix}. \tag{4}$$

**Algorithm 2** Primal-Dual Solver for Sub-Problem $\mathbf{argmin}_{\mathcal{S}}\, E(\mathcal{U}^k, \mathcal{S})$

Input: $\mathcal{U}^k$
Initialize $\mathcal{S}^0$
**for** $n = 0, 1, 2, ...$ **do**
$\mathcal{Q}(\boldsymbol{x})^{n+1} = \Pi_1 \left[\mathcal{Q}(\boldsymbol{x})^n + \tau \nabla \tilde{\mathcal{S}}(\boldsymbol{x})^n\right]$
$\mathcal{S}(\boldsymbol{x})^{n+1} = \Pi_3 \left[\mathcal{S}(\boldsymbol{x})^n - \sigma \left(\mathcal{U}(\boldsymbol{x})^k (\mathcal{C}(\boldsymbol{x}) - \mathcal{S}(\boldsymbol{x})^n \mathcal{U}(\boldsymbol{x})^k) - \nabla^\mathsf{T} \mathcal{Q}(\boldsymbol{x})^{n+1}\right)\right]$
$\tilde{\mathcal{S}}(\boldsymbol{x})^{n+1} = 2\,\mathcal{S}(\boldsymbol{x})^{n+1} + \mathcal{S}(\boldsymbol{x})^n$
**end for**

It calculates for each channel the derivative in $x$ and $y$ direction. The differential operators $\nabla_x$ $\nabla_y$ can be implemented using a difference scheme of choice. In our implementation we use forward differences. Since $\mathcal{S}$ is a single channel image, the gradient operator used in Algorithm 2 composes of a difference operator $\nabla_x$ and an operator $\nabla_y$ i.e: Which calculates for each channel the derivative in $x$ and $y$ direction. The differential operators $\nabla_x$ $\nabla_y$ can be implemented using a difference scheme of choice. In our implementation we use forward differences. Since $\mathcal{S}$ is a single channel image, the gradient operator used in Algorithm 2 composes of a difference operator $\nabla_x$ and an operator $\nabla_y$ *i.e.*:

$$\nabla = \begin{bmatrix} \nabla_x \\ \nabla_y \end{bmatrix}. \tag{5}$$

## 2. Evaluation

The following figures show additional results of our approach on real world scenes, which we recorded with a Kinect One. For every figure we show the input color image $\mathcal{C}$, the infrared albedo image $\mathcal{A}$ after fusion, our color albedo image $\mathcal{U}$, and our estimated shading image $\mathcal{S}$. As comparison we provide the results of the approach of Chen *et al*. [2]. We compute these results using their publicly available implementation.

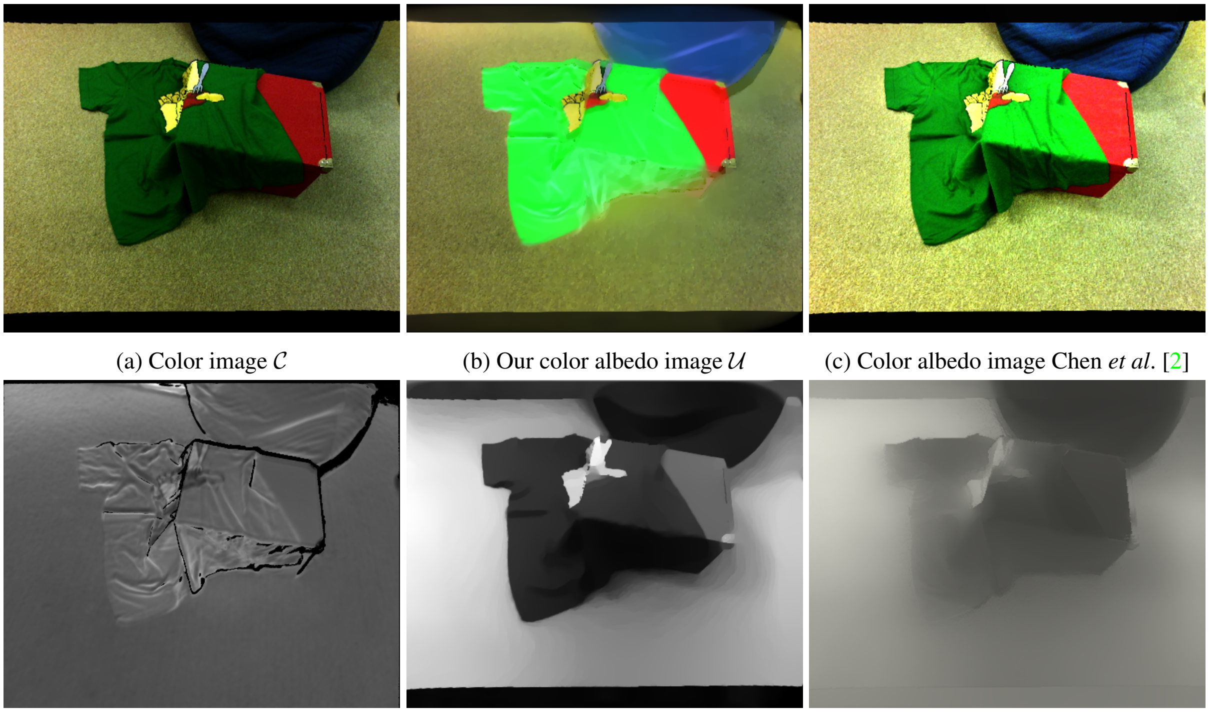

(a) Color image $\mathcal{C}$ (b) Our color albedo image $\mathcal{U}$ (c) Color albedo image Chen *et al.* [2]

(d) Infrared albedo image $\mathcal{A}$ (e) Our shading image $\mathcal{S}$ (f) Shading image Chen *et al.* [2]

Figure 1: Paper Figure 4 row 1

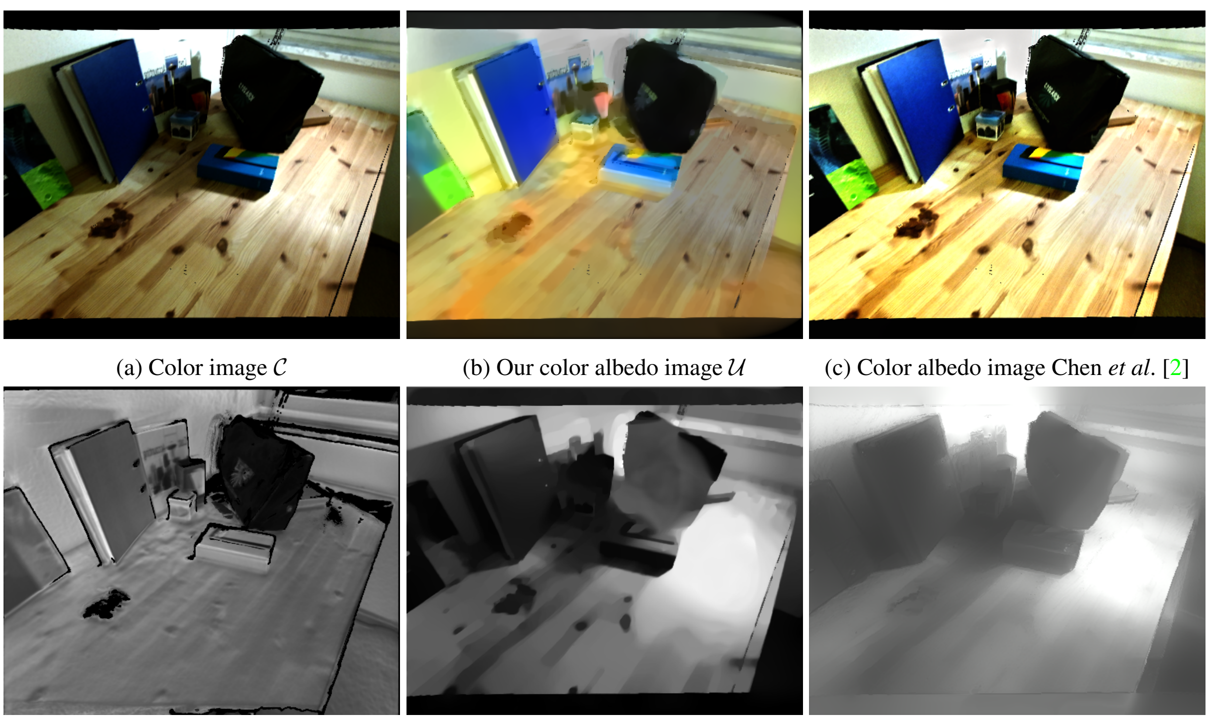

(a) Color image $\mathcal{C}$ (b) Our color albedo image $\mathcal{U}$ (c) Color albedo image Chen *et al.* [2]

(d) Infrared albedo image $\mathcal{A}$ (e) Our shading image $\mathcal{S}$ (f) Shading image Chen *et al.* [2]

Figure 2: Paper Figure 4 row 2

(a) Color image $\mathcal{C}$

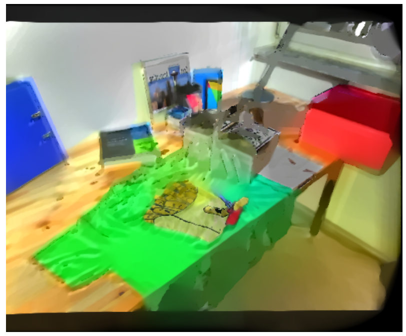

(b) Our color albedo image $\mathcal{U}$

(c) Color albedo image Chen *et al*. [2]

(d) Infrared albedo image $\mathcal{A}$

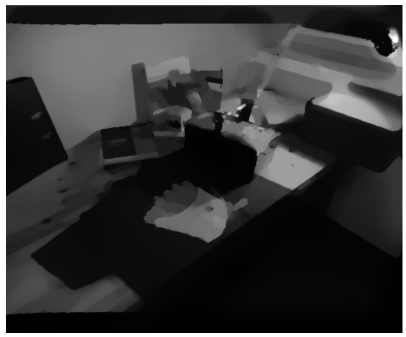

(e) Our shading image $\mathcal{S}$

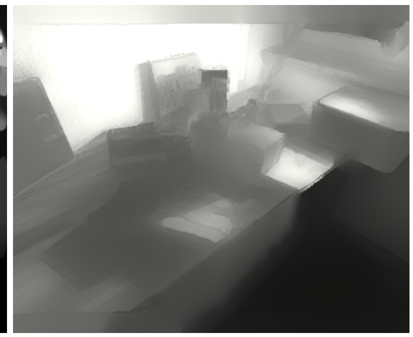

(f) Shading image Chen *et al*. [2]

Figure 3: Paper Figure 4 row 3

(a) Color image $\mathcal{C}$

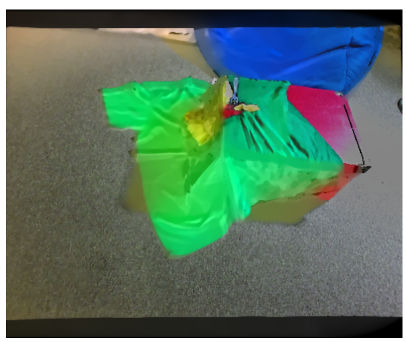

(b) Our color albedo image $\mathcal{U}$

(c) Color albedo image Chen *et al*. [2]

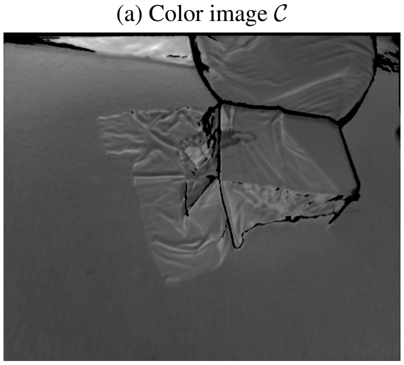

(d) Infrared albedo image $\mathcal{A}$

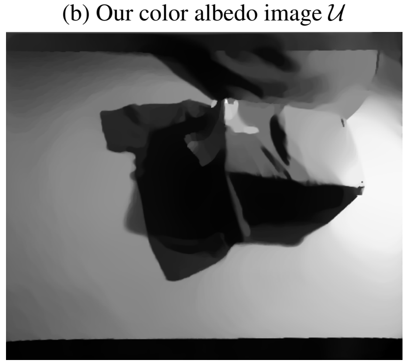

(e) Our shading image $\mathcal{S}$

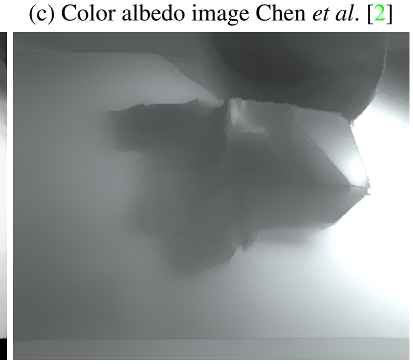

(f) Shading image Chen *et al*. [2]

Figure 4: Same scene as Figure 1 with additional spot light.

(a) Color image $\mathcal{C}$ (b) Our color albedo image $\mathcal{U}$ (c) Color albedo image Chen *et al.* [2]

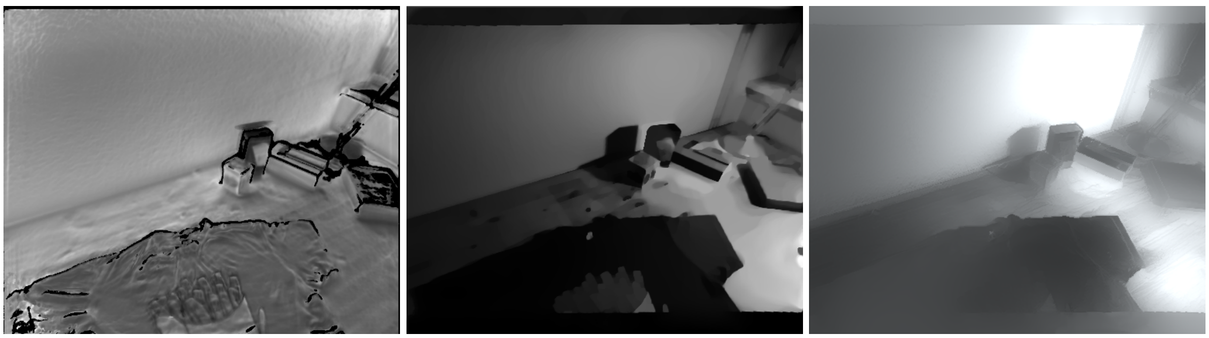

(d) Infrared albedo image $\mathcal{A}$ (e) Our shading image $\mathcal{S}$ (f) Shading image Chen *et al.* [2]

Figure 5: Desk scene with different objects. Note: our approach better removes shadows from the wall behind the boxes.

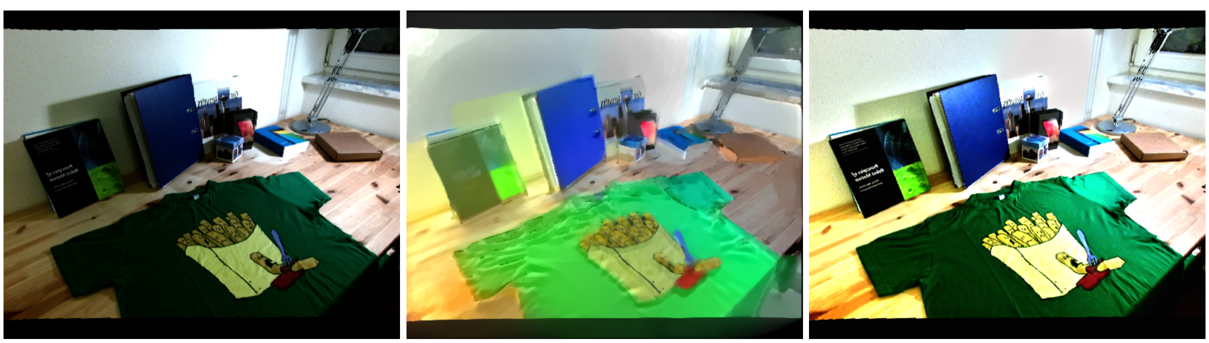

(a) Color image $\mathcal{C}$ (b) Our color albedo image $\mathcal{U}$ (c) Color albedo image Chen *et al.* [2]

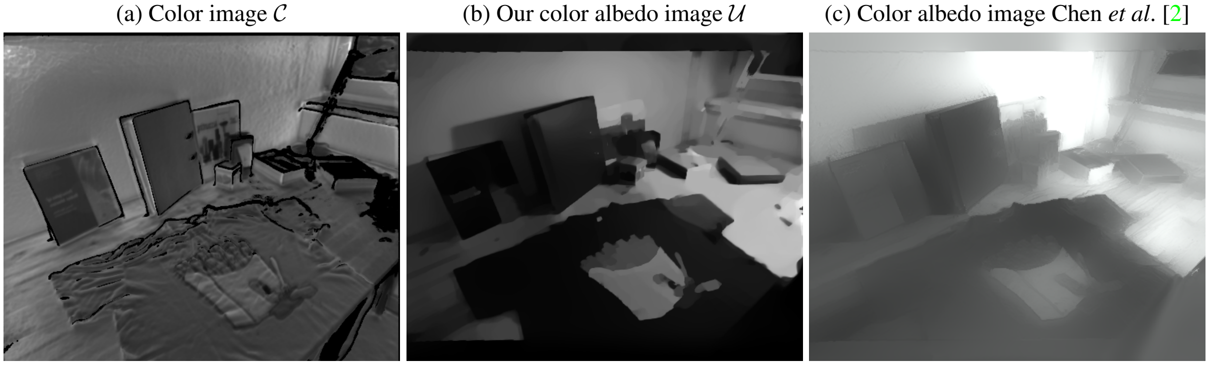

(d) Infrared albedo image $\mathcal{A}$ (e) Our shading image $\mathcal{S}$ (f) Shading image Chen *et al.* [2]

Figure 6: Desk scene

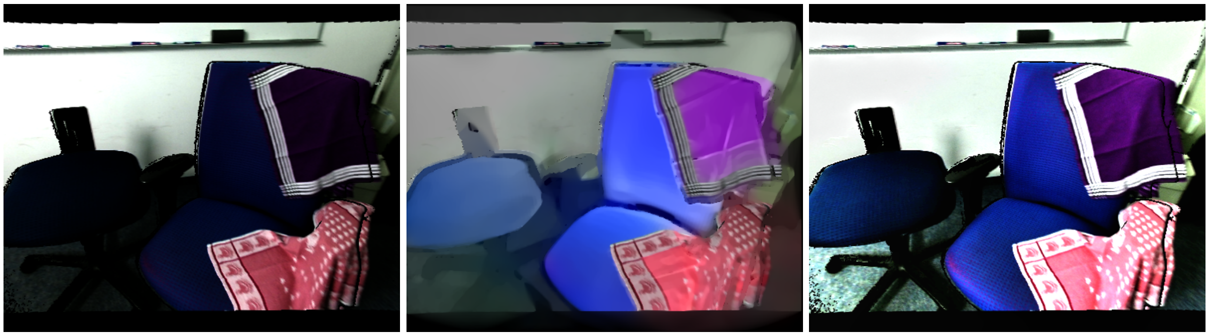

(a) Color image $\mathcal{C}$ (b) Our color albedo image $\mathcal{U}$ (c) Color albedo image Chen *et al*. [2]

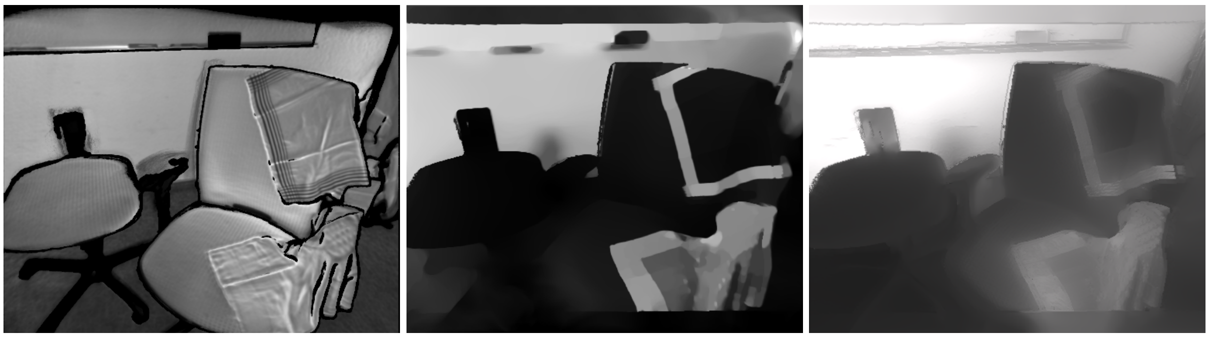

(d) Infrared albedo image $\mathcal{A}$ (e) Our shading image $\mathcal{S}$ (f) Shading image Chen *et al*. [2]

Figure 7: Chairs

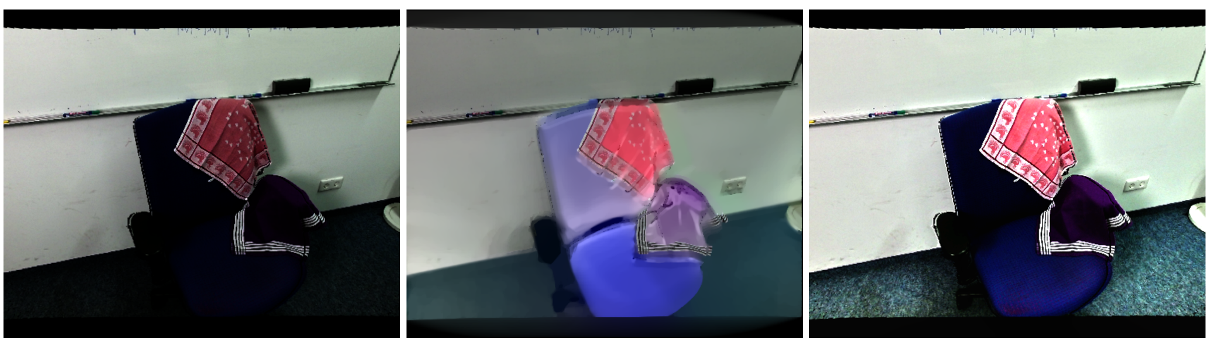

(a) Color image $\mathcal{C}$ (b) Our color albedo image $\mathcal{U}$ (c) Color albedo image Chen *et al*. [2]

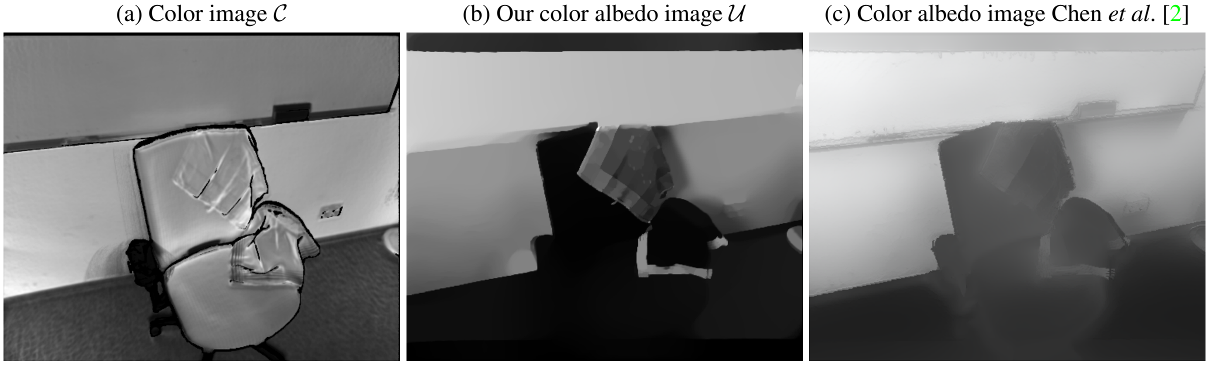

(d) Infrared albedo image $\mathcal{A}$ (e) Our shading image $\mathcal{S}$ (f) Shading image Chen *et al*. [2]

Figure 8: Chair

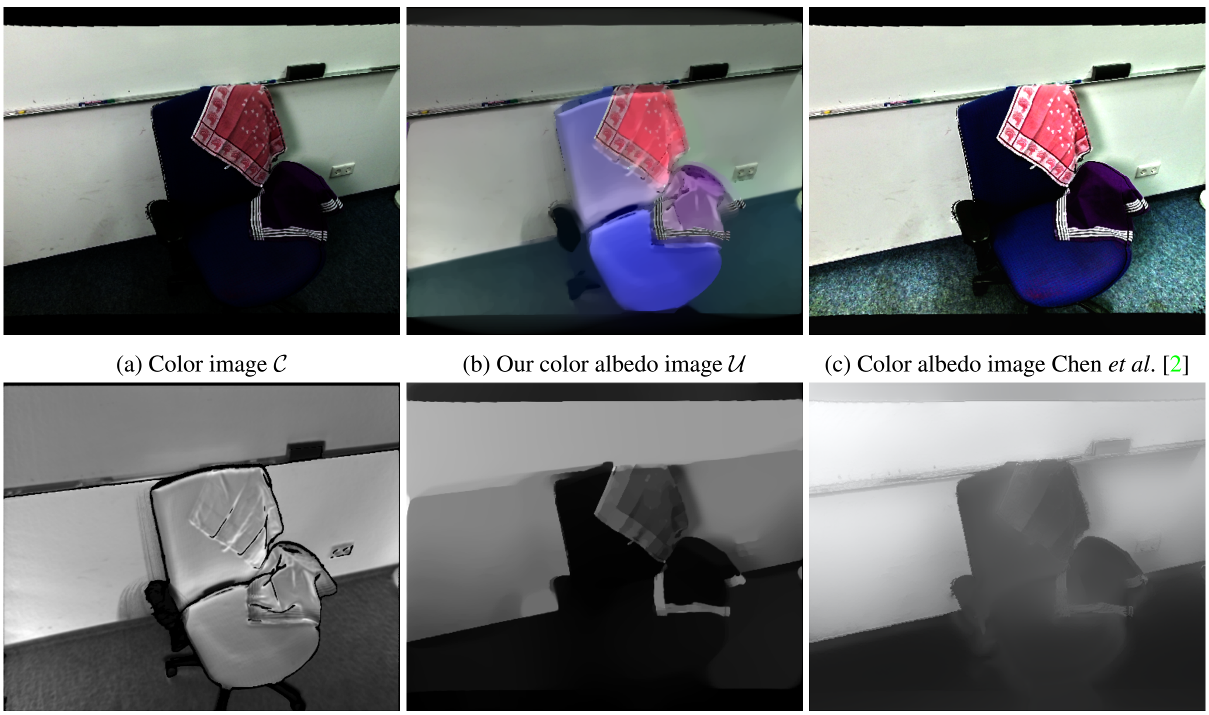

(a) Color image $\mathcal{C}$ (b) Our color albedo image $\mathcal{U}$ (c) Color albedo image Chen *et al*. [2]

(d) Infrared albedo image $\mathcal{A}$ (e) Our shading image $\mathcal{S}$ (f) Shading image Chen *et al*. [2]

Figure 9: Chair

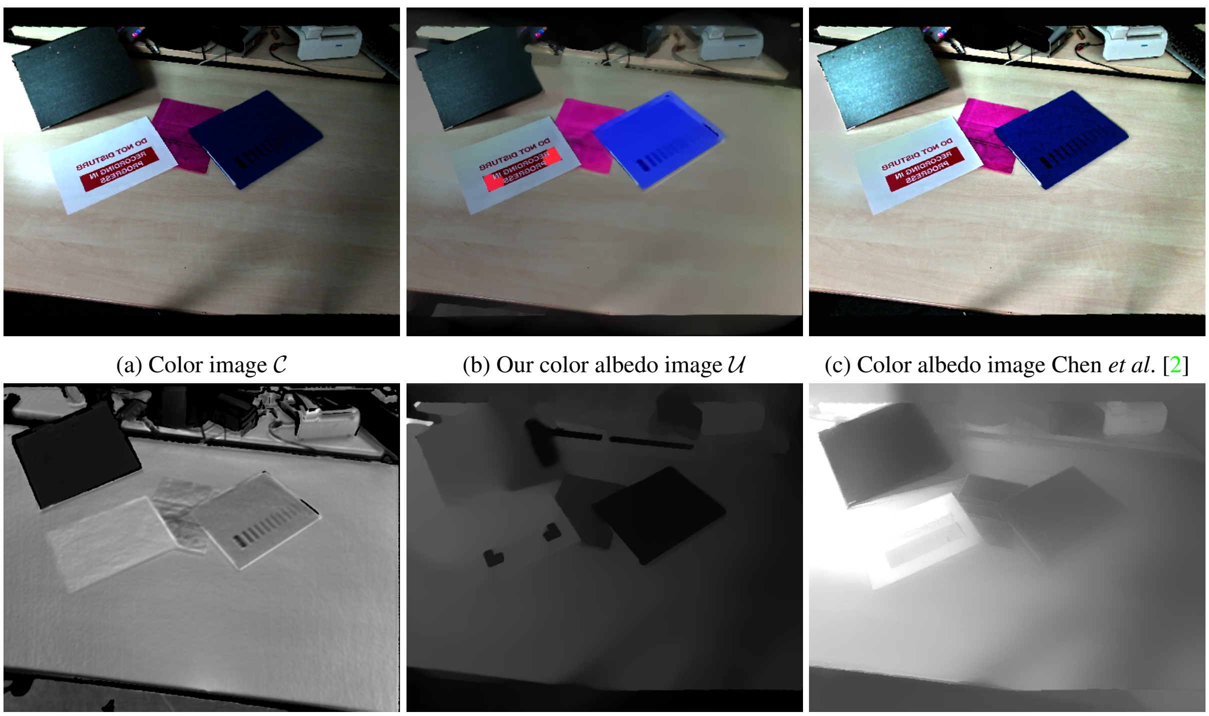

(a) Color image $\mathcal{C}$ (b) Our color albedo image $\mathcal{U}$ (c) Color albedo image Chen *et al*. [2]

(d) Infrared albedo image $\mathcal{A}$ (e) Our shading image $\mathcal{S}$ (f) Shading image Chen *et al*. [2]

Figure 10: Desk scene. Note that our algorithm maintains details in the color albedo image $\mathcal{U}$, which are not present in the infrared albedo image $\mathcal{A}$, *e.g.*, text on printed paper.

(a) Color image $\mathcal{C}$

(b) Our color albedo image $\mathcal{U}$

(c) Color albedo image Chen *et al*. [2]

(d) Infrared albedo image $\mathcal{A}$

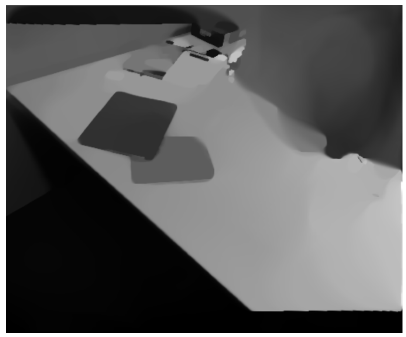

(e) Our shading image $\mathcal{S}$

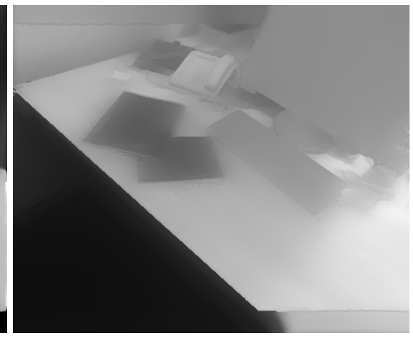

(f) Shading image Chen *et al*. [2]

Figure 11: Desk scene

(a) Color image $\mathcal{C}$

(b) Our color albedo image $\mathcal{U}$

(c) Color albedo image Chen *et al*. [2]

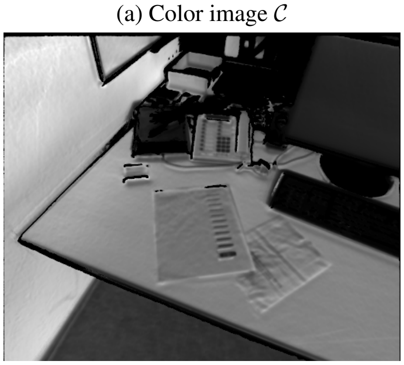

(d) Infrared albedo image $\mathcal{A}$

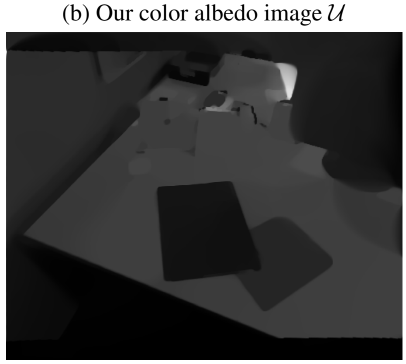

(e) Our shading image $\mathcal{S}$

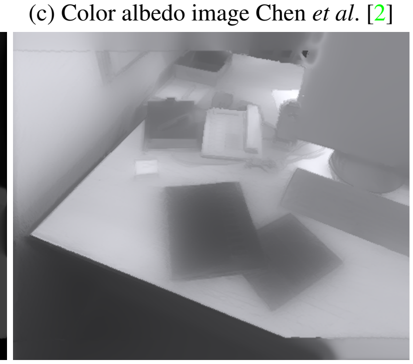

(f) Shading image Chen *et al*. [2]

Figure 12: Desk scene

(a) Color image $\mathcal{C}$ (b) Our color albedo image $\mathcal{U}$ (c) Color albedo image Chen *et al*. [2]

(d) Infrared albedo image $\mathcal{A}$ (e) Our shading image $\mathcal{S}$ (f) Shading image Chen *et al*. [2]

Figure 13: Stand

(a) Color image $\mathcal{C}$ (b) Our color albedo image $\mathcal{U}$ (c) Color albedo image Chen *et al*. [2]

(d) Infrared albedo image $\mathcal{A}$ (e) Our shading image $\mathcal{S}$ (f) Shading image Chen *et al*. [2]

Figure 14: Shelf

(a) Color image $\mathcal{C}$

(b) Our color albedo image $\mathcal{U}$

(c) Color albedo image Chen *et al*. [2]

(d) Infrared albedo image $\mathcal{A}$

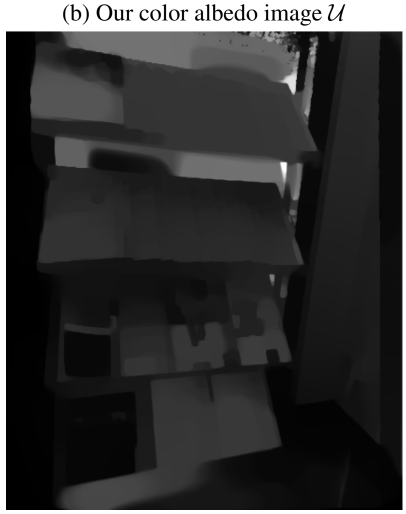

(e) Our shading image $\mathcal{S}$

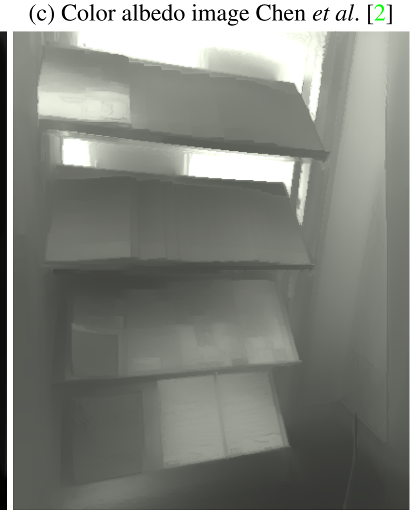

(f) Shading image Chen *et al*. [2]

Figure 15: Stand

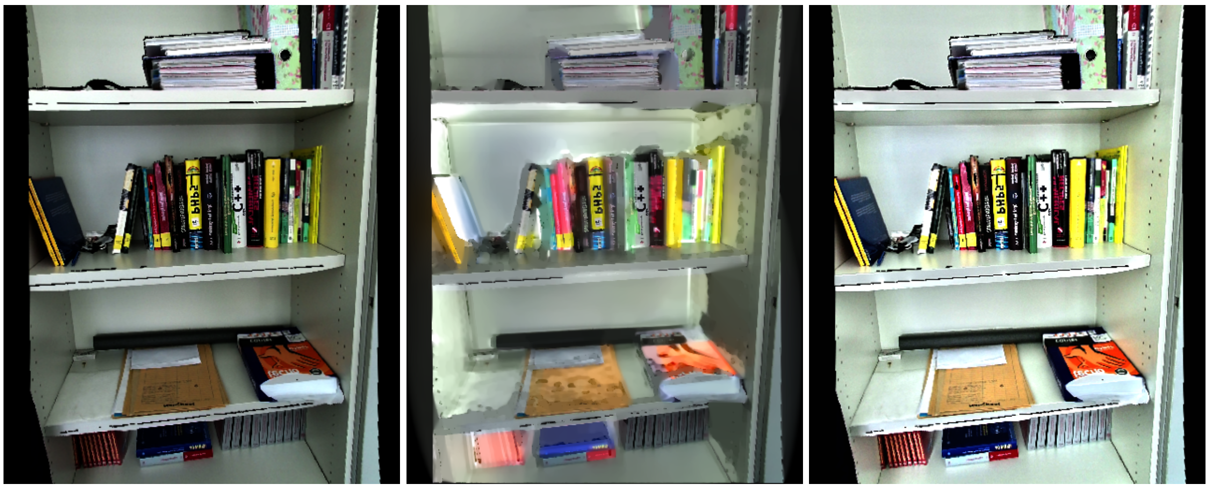

(a) Color image $\mathcal{C}$ (b) Our color albedo image $\mathcal{U}$ (c) Color albedo image Chen *et al*. [2]

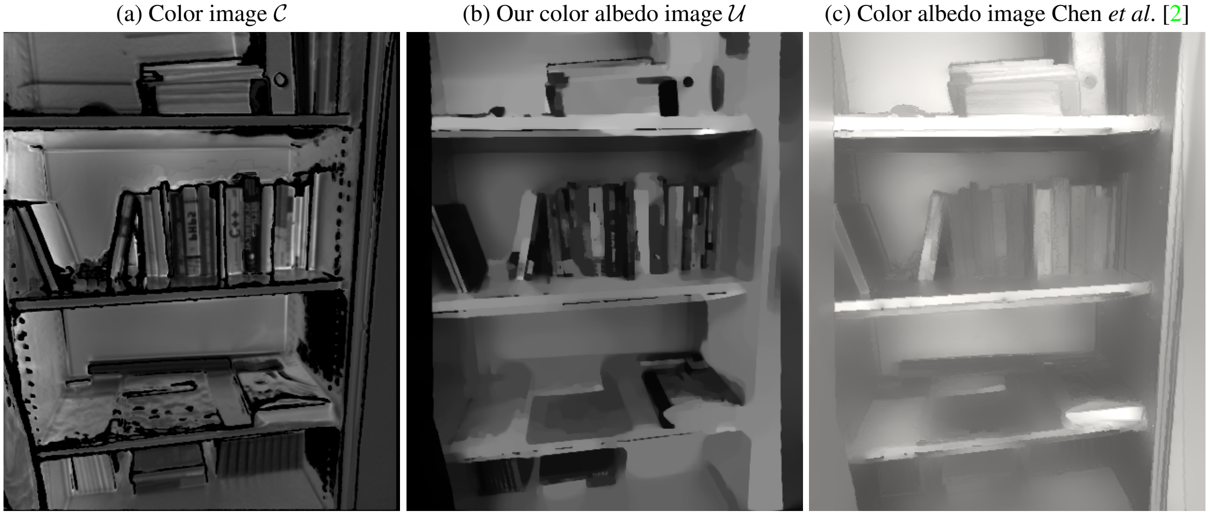

(d) Infrared albedo image $\mathcal{A}$ (e) Our shading image $\mathcal{S}$ (f) Shading image Chen *et al*. [2]

Figure 16: Book shelf

## References


[1] A. Chambolle and T. Pock. A first-order primal-dual algorithm for convex problems with applications to imaging. *JMIV*, 40(1):120–145, 2011. 1

[2] Q. Chen and V. Koltun. A simple model for intrinsic image decomposition with depth cues. In *Computer Vision (ICCV), 2013 IEEE International Conference on*. IEEE, 2013. 2, 3, 4, 5, 6, 7, 8, 9, 10, 11, 12, 13